The structure of epitaxial layers of uranium

2008 J. Phys.: Condens. Matter 20 135003

(http://iopscience.iop.org/0953-8984/20/13/135003)

J. Phys.: Condens. Matter **20** (2008) 135003 (9pp) doi:10.1088/0953-8984/20/13/135003

The structure of epitaxial layers of uranium

R C C Ward[1], R A Cowley[1,4], N Ling[1], W Goetze[1], G H Lander[2] and W G Stirling[3]

[1] Clarendon Laboratory, Oxford Physics, Parks Road, Oxford OX1 3PU, UK
[2] European Commission, JRC, Institute for Transuranium Elements, Postfach 2340, D-76125 Karlsruhe, Germany
[3] European Synchrotron Radiation Facility, BP220, F-38043, Grenoble, Cedex 09, France

E-mail: r.cowley@physics.ox.ac.uk

Received 30 November 2007, in final form 6 February 2008
Published 4 March 2008
Online at stacks.iop.org/JPhysCM/20/135003

Abstract
Epitaxial layers of uranium have been grown on a variety of buffer/seed layers on sapphire substrates by UHV magnetron sputtering and their structure determined using x-ray diffraction. The buffer layers were epitaxial layers of niobium, tungsten and niobium covered by a seed layer of hcp gadolinium, on which uranium layers were grown to a thickness of 600 Å. The x-ray diffraction results establish that the α-orthorhombic phase of uranium grows epitaxially in the (110) orientation on the niobium (110) buffer, while on the tungsten (110) buffer the growth planes of the α-uranium were (002) and for the growth on the gadolinium buffer the α-uranium was predominantly (021) oriented. These results show that epitaxial uranium films in selected orientations can be grown by using an appropriate buffer. To our knowledge this is the first report of epitaxial α-uranium films, and it is significant because of the difficulty of growing single crystals of α-uranium due to the occurrence of high temperature structural transformations.

(Some figures in this article are in colour only in the electronic version)

1. Introduction

We shall show in this paper that epitaxial thin films of uranium can be grown using the technique of UHV magnetron sputtering. This is important for three reasons. Firstly the structure of uranium metal in thin films is controversial and has been reported as possibly hexagonal close packed, whereas the structure of the bulk is orthorhombic. Secondly theoretical calculations of the 5f actinides predict different structures, some of which are magnetic while others have charge density wave instabilities. Thirdly it is difficult to test these predictions by either scattering measurements or conventional bulk measurements without single crystal samples, which cannot be grown by conventional methods because of two high temperature phase transitions. Single crystals are also required for surface measurements to investigate, for example, in detail how uranium is leached when stored for a long time.

Above a temperature of 1045 K, uranium has the body-centred cubic structure, which on cooling transforms to the β form, which has a complex tetragonal structure. On further cooling below 940 K the structure is an unusual orthorhombic structure known as the α-uranium structure, which is then stable down to the lowest temperature, apart from a transition at 43 K involving a charge density wave. Because of the two drastic phase changes that occur at about 1000 K it is impossible to grow single crystals of uranium using conventional slow solidification methods.

We have used conventional UHV sputtering techniques with controlled substrate temperature to obtain single crystal samples of uranium. Since the growth occurs at temperatures considerably below 1000 K the samples grow directly in the low temperature structure and so the samples do not have to be cooled through the two reconstructive high temperature phase transitions. In addition, single crystal growth of thin films of uranium on different substrates holds out the possibility of being able to change the electronic state of the electrons from a state in which the electrons are itinerant, as in bulk uranium metal, to one in which they are localized, as in uranium dioxide, by varying the U–U distance. We show

[4] Author to whom any correspondence should be addressed.

that by growing the thin films on various different substrates we obtain the bulk structure, orthorhombic α-uranium, but in different orientations.

There have been other experiments that have reported the growth of uranium thin layers. Molodtsov *et al* report [1] that they have grown uranium layers on a cooled tungsten (110) surface to a thickness of 80 Å. The uranium was not ordered in the plane of the layers. After annealing at 1400 K they were able to obtain a more ordered layer structure that was shown by LEED measurements to be either a hexagonal structure or several domains of a face-centred cubic structure. They measured the photoemission and compared the measurements with calculations of the electronic structure. More recently, Berbil-Bautista *et al* [2] have grown uranium layers again on cooled tungsten (110) planes with a thickness of about 80 Å, which were then annealed at 800 K. They used scanning tunnelling spectroscopy to measure the surface structure, which was suggested to be hexagonal with a similar in-plane lattice constant to that found by Molodtsov *et al*. The spectroscopic measurements were then compared with the result of band structure calculations. Note that these previous reports of epitaxial uranium involved exclusively *in situ* surface analysis to determine the structure of the thin films. Full *ex situ* x-ray diffraction was not possible because the thin films were less than 100 Å in thickness. To our knowledge there have been no previous reports of epitaxial α-uranium films.

Other measurements have been made in Oxford, in a prototype of the present growth facility, of multilayers of uranium/iron and uranium/gadolinium [3–5]. These samples were grown to study whether the large ferromagnetic moments on the iron or the gadolinium would induce magnetic moments on the uranium layers. As they were grown at room temperature, the materials did not grow with an epitaxial layer structure and hence it was very difficult to determine the crystal structure of the layers. However, in the case of U/Gd multilayers [4], the uranium plane spacing in the growth direction, as well as RHEED measurements, suggested that the uranium might be in a hexagonal phase.

Recent improvements to the Oxford sputtering facility, in particular by the introduction of a high temperature substrate stage, have enabled samples of uranium to be grown with greatly improved structures and in particular with ordered in-plane structures. As a result we have embarked on a programme of studying the structure of epitaxial uranium layers when grown on various different substrates and under different conditions. The layers were grown to a thickness of 600 Å so that the structures could be easily determined using the x-ray facilities available in Oxford. The next section describes firstly the growth facility and the procedures used and secondly the x-ray facilities and the measurements made.

In section 3 we shall describe the results of growing uranium layers on niobium, tungsten and then niobium followed by gadolinium. We demonstrate that for all three substrates we obtain the α-uranium structure but with different orientations. The (110) niobium substrate gives (110) uranium growth planes, the (110) tungsten gives largely the uranium (002) growth planes while the gadolinium gives growth of both (110) and (021) uranium planes. Finally, in the fourth section we summarize and discuss our results.

2. Experimental methods

2.1. Growth of uranium layers

The uranium films were grown in a dedicated DC magnetron sputtering facility with UHV base pressure, *in situ* RHEED analysis and substrate heating to 1070 K. Substrates were single crystal sapphire of (11.0) orientation and polished commercially to 'epitaxial polish' specification. Prior to loading into the UHV growth facility, the substrates were degreased by boiling successively in trichloroethylene, propan-2-ol and methanol. Immediately prior to film deposition the substrates were UHV annealed in the growth chamber at 1070 K for 30 min.

Buffer layers of niobium or tungsten were employed and were deposited onto the sapphire substrates at 1070 K. At elevated temperatures the bcc refractory metals are well known to grow epitaxially in the (110) orientation on sapphire (11.0). This was confirmed in the present study, with an added complexity in the case of tungsten that two tungsten domains were found, which were related by a 70° in-plane rotation corresponding to alignment of the in-plane $[1\bar{1}1]$ and $[\bar{1}11]$ axes of tungsten parallel to the [00.1] sapphire axis. In contrast, niobium was always found to grow with a single domain [6]. The sapphire/refractory metal substrate system has been used widely and successfully in the past for epitaxy of rare earth and transition metal structures, and so was an obvious candidate for the growth of epitaxial uranium.

Uranium was sputtered onto the niobium (110) or tungsten (110) buffer surfaces at a temperature of 870 K in an argon pressure of 5×10^{-3} mbar and a growth rate of 0.5–1 Å s^{-1}. In an additional experiment, a seed layer of gadolinium was inserted between the niobium and uranium layers. This was motivated by the results from our previous U/Gd multilayer samples grown at room temperature [4], which showed evidence of the uranium taking up a hexagonal structure. After RHEED analysis, all the samples were capped with a thin layer of the refractory metal to preserve the uranium layer from atmospheric attack for the *ex situ* experiments.

The details of the growth conditions and mosaic spreads for the different samples are listed in table 1.

2.2. X-ray scattering measurements of the structure

The x-ray measurements were made in Oxford with a PANalytical MRD Diffractometer, which had a Cu x-ray tube followed on the incident x-ray side by a four bounce (220) Ge monochromator and a curved focusing mirror. On the scattered side we used either a three bounce Ge (220) analyser or for most of the experiments a slit with a 1/4° angular acceptance in the horizontal plane. This gives a very elongated resolution function in the direction perpendicular to the scattered wavevector; this is not a problem measuring the broad uranium scattering, but is a problem measuring the very sharp sapphire scattering. The vertical divergence perpendicular to the scattering plane was determined by slits and was about 3.0°.

After alignment of the samples in the horizontal scattering plane, the first measurements made were with the wavevector

Table 1. Growth of uranium layers.

Sample	Nb/W growth temp. (°C)	Nb/W mosaic spread (deg.)	Gd growth temp. (°C)	Gd mosaic spread (deg.)	U growth temp. (°C)	U mosaic spread (deg.)
Nb–U	800	0.17 ± 0.01			600	0.15 ± 0.01
W–Nb	800	0.13 ± 0.01			600	0.15 ± 0.01
Nb–Gd–U	800	0.08 ± 0.01	600	0.50 ± 0.02	600	0.72 ± 0.03

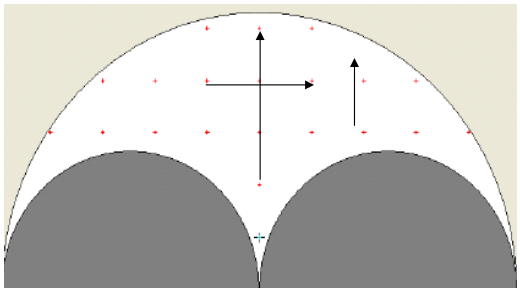

Figure 1. The diagram shows the reciprocal lattice of a crystal, with the regions which cannot be measured in black or grey. The on-axis longitudinal scan is made from the origin vertically and the off-axis scan is made with the wavevector making a parallel line but displaced from the origin. A transverse scan is horizontal in the diagram.

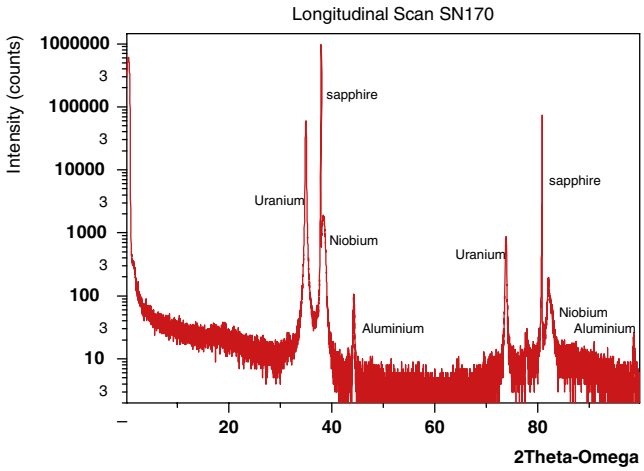

Figure 2. A longitudinal scan parallel to the growth axis showing two sets of reflections from the sapphire, niobium and uranium. This scan was performed for all the samples, although only the most intense part is shown in the remaining diagrams.

transfer along the growth direction, which we call a longitudinal scan or a 2θ–Ω scan, with $\Omega = \theta$, as shown in figure 1. This type of scan determines the plane spacing along the growth direction. A transverse scan perpendicular to the growth direction determines the mosaic spread. The structure and orientation of the layer planes require the measurement of an inclined (off-axis) Bragg reflection. These reflections are more difficult to measure because the substrate of the sample is not transparent to x-rays and so the sample orientation Ω must be between 0° and 2θ for both incident and scattered beams to pass through the front face of the sample, as shown in figure 1. In practice, a particular off-axis reflection was chosen and the angles set up for observing this reflection. We then adjusted the rotation of the sample about the growth axis, ϕ, until a reflection was found. The zero of the ϕ angle depends on the way the sample is mounted on the diffractometer and so only the relative angles are significant. A full rotation about ϕ shows the angles at which the reflections occur and the angles between the peaks provides information to identify the structure or structures of the layers. In this paper we shall show either longitudinal on-axis scans along the growth direction or ϕ scans to show the orientation and existence of off-axis reflections. When this procedure is used for each of the different layers in the sample the relative orientations of the different layers can be deduced. This procedure is simple as explained above, but in practice the sample needs to be very accurately aligned if similar peaks in the ϕ scan are to be observed to have the same intensity, while the different layers also need to be parallel with one another. Nevertheless, reasonably accurate results can be obtained provided that care is taken in interpreting the results, as pointed out in section 3.

3. Experimental XRD results

3.1. Niobium/uranium

Longitudinal on-axis scans, for example figure 2, showed peaks at the intense narrow sapphire reflections (11.0) and (22.0) at wavevector transfers $Q = 2.646 \pm 0.002$ Å^{-1} and 5.289 ± 0.002 Å^{-1}, peaks corresponding to the niobium reflections (110) and (220) at wavevector transfers of 2.680 ± 0.002 Å^{-1} and 5.356 ± 0.002 Å^{-1} and further peaks from the uranium film at 2.450 ± 0.002 Å^{-1} and 4.900 ± 0.002 Å^{-1}. These last reflections can be compared with the wavevectors of the reflections for bulk α-uranium in table 2 and strongly suggest that these uranium reflections are from α-uranium (110) and (220) reflections respectively. The mosaic spread of lowest angle reflections was measured as $0.15 \pm 0.01°$, which is slightly smaller than the mosaic spread of the niobium buffer, $0.17 \pm 0.01°$.

The orientation of the niobium planes was determined from the positions of the niobium (310) reflections obtained by rotating the sample about the growth direction using the angle ϕ. Two (310) reflections were found per 360° rotation, and these were measured to be 180° apart, and at an angle of approximately 35° from the sapphire [00.1] direction as indicated from the sides of the sapphire substrate. This is the normal sapphire/niobium epitaxial relationship, $Al_2O_3(11.0)[00.1] \parallel Nb(110)[1\bar{1}1]$, and only one orientation of the niobium layer is formed on the sapphire substrate [6].

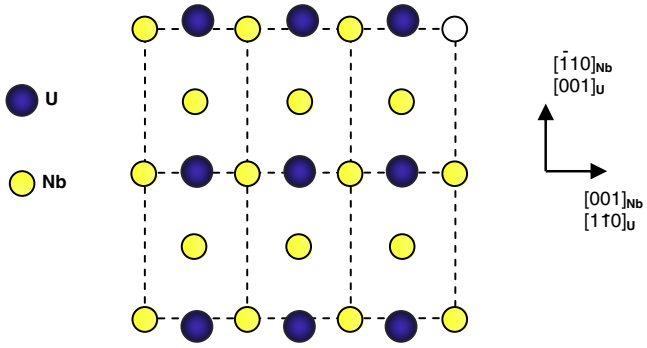

Figure 3. Schematic diagram of the epitaxial relationships between Nb and U.

Table 2. Structure of bulk α-uranium [7]. Cell and symmetry information: space group, $Cmcm$; lattice parameters, $a = 2.854$, $b = 5.87$, $c = 4.955$; reciprocal lattice parameters $a^* = 2.201$, $b^* = 1.070$, $c^* = 1.268$. Low angle Bragg reflections.

h	k	l	Q (Å^{-1})	2θ (deg.)
0	2	0	2.141	30.45
1	1	0	2.448	34.95
0	2	1	2.488	35.54
0	0	2	2.536	36.25
1	1	1	2.7569	39.53

The orientation of the uranium layer and confirmation of the (110) growth plane were obtained by measuring the ϕ orientation of the following off-axis Bragg reflections (221), (222), (223) and (240). The first three of these can be found easily because the [001] direction is perpendicular to the [110] direction, while the last is more complicated because the $[1\bar{1}0]$ direction is not perpendicular to the [110] direction in the orthorhombic structure of α-uranium. The results showed that the reciprocal lattice vector along the [001] direction was perpendicular to the growth direction and of length 1.271 ± 0.005 Å^{-1}, very close to that of the c axis of bulk α-uranium, as shown in table 2. For each reflection only two peaks were observed in a rotation of angle ϕ by 360°, and the α-uranium [001] direction was the same as the niobium $[1\bar{1}0]$ direction, which has a reciprocal lattice distance 2.692 ± 0.010 Å^{-1}. This reciprocal lattice parameter is approximately double the α-uranium reciprocal lattice vector along the c-axis. This orientation of a niobium and a uranium layer is shown in figure 3 in real space with a suggestion as to the relative position of the two layers. It is clear that there is a reasonably well defined fit between the planes in the niobium and uranium for this orientation. In more detail the (240) reflections of uranium occur with the ϕ angle 90° different from that of the (223) reflections. The wavevector distance of the (240) reflection from the (330) on-axis reflection is a Bragg reflection $(\bar{1}10)$ and was found to have a wavevector of $(-1.88, 1.49, 0)$, which is a length of 2.40 ± 0.02 Å^{-1} at an angle of $51.60 \pm 0.05°$ from the [110] direction. This result shows that the reciprocal lattice spacing perpendicular to both the [110] and [001] directions, 1.88 Å^{-1}, is, at least approximately, half the corresponding (002) wavevector for niobium, 3.81 Å^{-1},

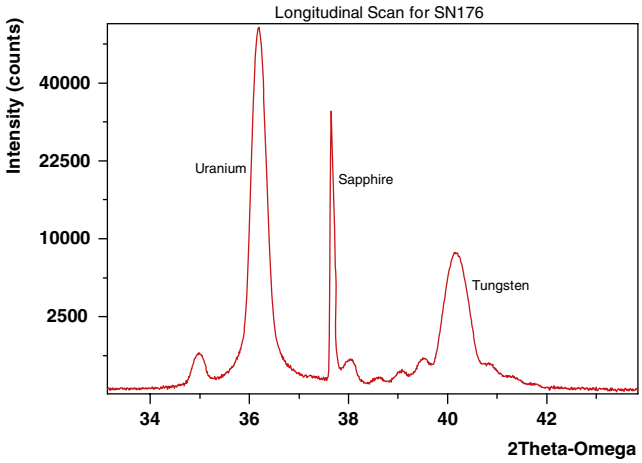

Figure 4. A restricted part of the longitudinal scan for sapphire, tungsten and uranium. The tungsten peak shows size fringes, while the peak on the rhs of the sapphire arises from an aluminium powder peak and the uranium shows two distinct peaks as described in the text.

Table 3. Reciprocal plane spacing for niobium and tungsten (110) planes and for gadolinium (00.2) and (10.0) planes, respectively.

Material	Sample	Between the growth planes (Å)	In the growth planes (Å)
Nb	Nb/U	2.354 ± 0.002	2.334 ± 0.010
	Nb/Gd/U	2.324 ± 0.002	2.370 ± 0.010
	Bulk Nb	2.334	2.334
W	W/U	2.241 ± 0.002	2.234 ± 0.010
	Bulk W	2.238	2.238
Gd	Nb/Gd/U	5.780 ± 0.003	3.637 ± 0.010
	Bulk Gd	5.784	3.637

and demonstrates that the α-uranium has grown epitaxially on the underlying niobium buffer layer with relatively little strain of the α-uranium. This behaviour of the buffer and uranium layers is described in tables 3 and 4, respectively, and is shown schematically in figure 3. The structure shown in figure 3 is schematic because we have no information about the relative position of the niobium and uranium lattices, although we know the orientation of both lattices.

3.2. Tungsten/uranium

Similar measurements were made for a uranium layer grown on a tungsten buffer under the conditions shown in table 1. This experiment was conducted because earlier studies [1, 2] used a tungsten metal substrate and reported the growth of a hexagonal form of uranium, and we wished to discover if we also obtained this structure when we used a tungsten buffer. The scattering observed from a scan with the wavevector parallel to the growth axis of uranium on a sample with a tungsten buffer is shown in figure 4. The peak from the sapphire substrate (11.0) is the narrowest reflection and occurs at a wavevector $Q = 2.634 \pm 0.010$ Å^{-1}, while the (22.0) reflection is at a wavevector of 5.2753 ± 0.010 Å^{-1}, as expected. The peak from the tungsten occurs at

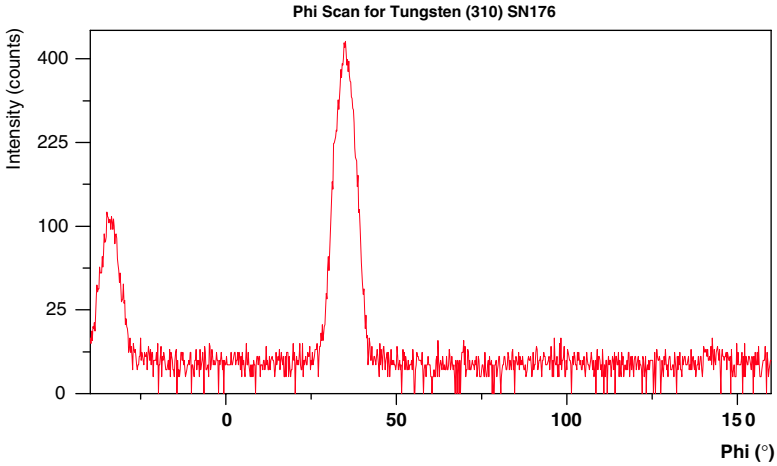

Figure 5. A part of the ϕ scan for the tungsten (310) reflection. Each peak corresponds to a different domain and the one at the smaller angle has the smaller intensity.

Table 4. Reciprocal lattice parameters and orientation of uranium layers.

Sample	Growth direction	Lattice parameter ($Å^{-1}$)	In-plane direction	Lattice parameter ($Å^{-1}$)	Orientation parallel to
Nb/U	[110]	2.450 ± 0.002	[001]	1.271 ± 0.010	Nb[1$\bar{1}$0]
			[1$\bar{1}$0]	2.400 ± 0.020	Nb[001]
W/U	[002]	2.530 ± 0.002	[110]	2.385 ± 0.010	W[111]
Nb/Gd/U	[021]	2.494 ± 0.005	[200]	4.382 ± 0.010	Gd[10.0]
			[001]	1.254 ± 0.010	
	[110]	2.450 ± 0.002	[001]	1.270 ± 0.010	Gd[10.0]

2.804 ± 0.010 $Å^{-1}$, in agreement with the expected tungsten (110) reciprocal lattice parameter, 2.8078 $Å^{-1}$. There are then two other peaks that are associated with the uranium. One occurs at 2.5277 ± 0.002 $Å^{-1}$ and the other is 140 times weaker and occurs at a wavevector of 2.4430 ± 0.002 $Å^{-1}$. The strongest of these reflections agrees with the wavevector of the (002) Bragg reflection of α-uranium while the weaker reflection agrees with the wavevector of the (110) Bragg reflection of α-uranium. Since this latter peak arises probably from the same structure as that discussed above in section 3.1, and also because the reflection was less than 1% of the strong Bragg reflection, we shall not discuss it further. Transverse scans were performed to determine the width of the different reflections, and the width of the tungsten (110) reflection was $0.13 \pm 0.01°$ and that of the uranium reflection was $0.148 \pm 0.015°$. These are very satisfactory values for sputtered layers.

The (110) Bragg reflection of the tungsten was measured as 2.804 ± 0.0020 $Å^{-1}$, while that of the (220) reflection gave 5.6053 ± 0.0030 $Å^{-1}$; both are slightly smaller than the reciprocal lattice vector of bulk tungsten. Measurements were made of the (310) off-axis Bragg reflection so as to determine the orientation of the buffer layer. The results are shown in figure 5, which surprisingly shows two domains as a function of the ϕ angle. One of the domains is at an angle of $\phi = -34.5°$ while the other has an intensity of about a factor of four times larger and is at 35.0°, where the error on both of these angles is 0.5°. This result shows that, unlike the case of niobium, which always has only one domain when grown on sapphire (11.0), tungsten has two possible domains orientated at approximately $\pm 35°$ from the sapphire [0001] direction but with a smaller amount of the domain that is the absent domain for niobium.

It was suggested above that the structure of the uranium layer was the alpha form with the (002) planes perpendicular to the growth axis. In order to confirm this result and to determine the orientation of the layers, the off-axis (024) Bragg reflections were studied and the results are shown in figure 6. The ϕ-scans unexpectedly showed three peaks, at $-26°$, 27° and 97°, suggesting that there are at least three different domains formed in the uranium layer. Measurements were then made of the intensities of the (114) Bragg reflections as the sample was rotated about the ϕ axis. A total of ten reflections were observed when ϕ was varied by 360° and these were classified as strong, medium or weak. In figure 7 we suggest the orientation of the different domains that could be identified from these results and how they are compatible with the observations of the intensities for the uranium (024) planes and the tungsten (310) reflections. The governing relationship in the epitaxy for these domains is that an in-plane $\langle 110 \rangle$ direction in uranium should be parallel to a $\langle 111 \rangle$ direction in the tungsten buffer, following the principle of matching of close-packed rows of atoms in the interface between the two lattices. In figure 7 the two tungsten domains are shown by the yellow and orange sets of atoms. For both of these tungsten domains one of the $\langle 111 \rangle$ directions is parallel to the sapphire [00.1] direction while the other $\langle 111 \rangle$ direction is at an angle

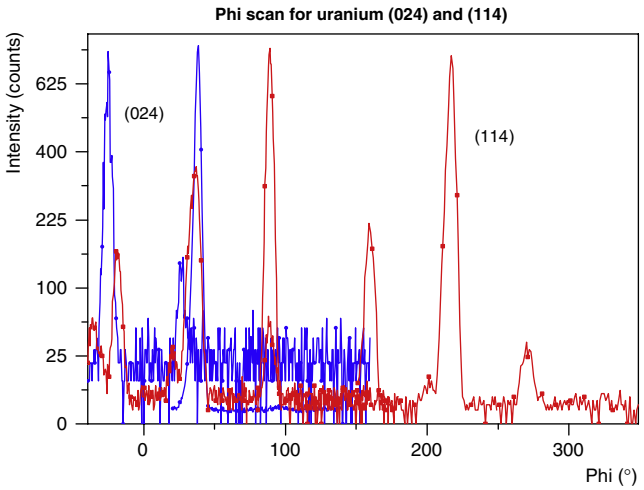

Figure 6. A part of the ϕ scan for the (024) reflection and the (114) reflections. Due to a slight misalignment of the sample it was necessary to realign the sample to obtain the full intensity of each peak so that, particularly for both reflections, the results are the sum of several scans.

of 70° away, and for one domain this rotation is clockwise and for the other it is anti-clockwise. In the uranium (002) plane there are two ⟨110⟩ directions, namely [110] and [$1\bar{1}0$], but, as we saw above, these two directions are not at right angles but 53° apart. Consequently, there are eight different possible U domains which fulfil the criterion U⟨110⟩ ∥ W⟨111⟩. These are shown in figure 7, and the close matching between the spacings of the U⟨110⟩ and W⟨111⟩ atomic rows is evident. It is this close match which drives the epitaxy. However, note that two pairs of U domains turn out to be equivalent (upper part of figure 7), so that there is actually a total of six independent U domains (two in the upper part of figure 7 and the four shown in the lower part).

In the experiment we observe the two domains with the [$1\bar{1}1$] direction of tungsten parallel to the sapphire [00.1] direction and these give the strongest scattering. Considerably weaker scattering is seen from the two domains that have the [110] directions almost perpendicular to the sapphire [00.1] direction, while the third pair of reflections with the uranium [110] directions at about 40° from the sapphire were not observable.

In more detail the tungsten off-axis (310) reflections had a transverse wavevector of 2.812 ± 0.010 Å^{-1}, which is slightly larger than the longitudinal wavevectors. The uranium (024) reflections had a transverse wavevector of 2.145 ± 0.015 Å^{-1}, which is in excellent agreement with the wavevector expected from α-uranium. The transverse reciprocal lattice vector of the (114) Bragg reflections was 2.385 ± 0.010 Å^{-1}, which is somewhat smaller than the (110) lattice vector of bulk α-uranium, as found in section 3.1. The angle between the [110] and [$\bar{1}10$] directions was on average 51.8±0.8° for the domains shown in the upper part of figure 7, which is very close to the bulk value of α-uranium, 51.9°. The angle between the [110] and [020] directions was found to be 63.3 ± 0.8°, which can be compared with the value of the angle in the bulk, 64.1°. The domains illustrated in the lower part of figure 7 were more distorted and the angle between the [110] and [$1\bar{1}0$] directions was 56.3±0.8°. Nevertheless, the [020] direction was observed

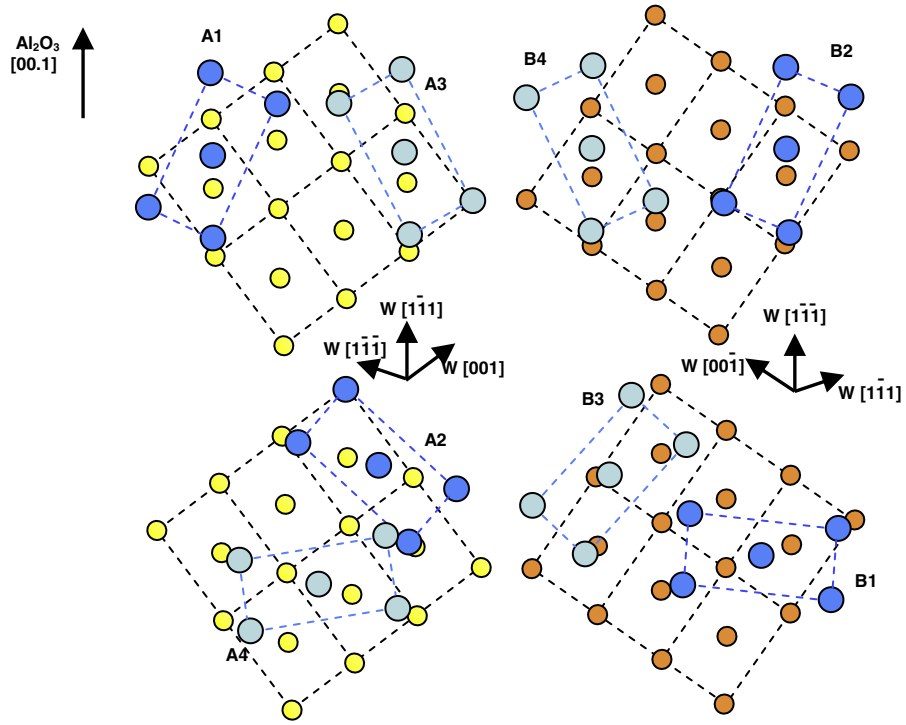

Figure 7. A schematic diagram of the epitaxial relationship between W and U showing the origin of the differently oriented domains. There are two W domains with the relationships for domain A $W[1\bar{1}1]$ ∥ Al_2O_3 [00.1] and for domain B $W[1\bar{1}\bar{1}]$ ∥ Al_2O_3 [00.1]. The four uranium domains have domain 1 $U[1\bar{1}0]$ ∥ $W[1\bar{1}\bar{1}]$, domain 2 $U[1\bar{1}0]$ ∥ $W[1\bar{1}\bar{1}]$, domain 3 $U[110]$ ∥ $W[1\bar{1}1]$ and domain 4 $U[110]$ ∥ $W[1\bar{1}\bar{1}]$.

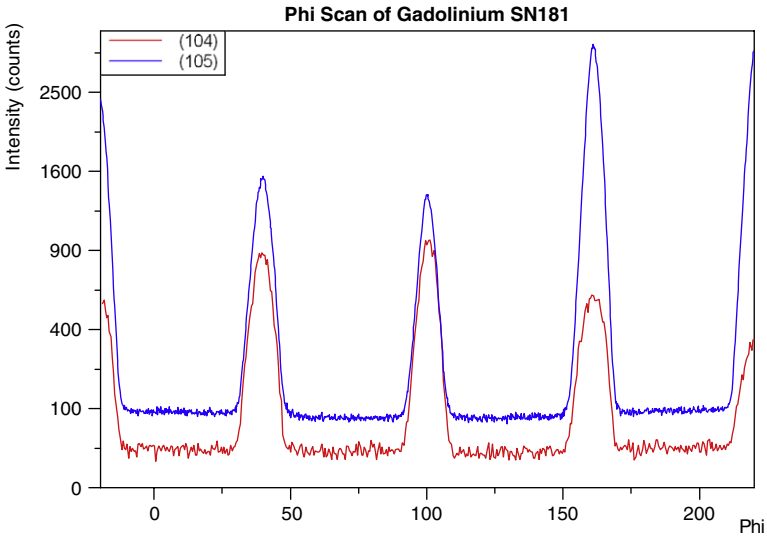

Figure 8. A ϕ scan of the gadolinium (10.4) and (10.5) reflections showing the hexagonal symmetry.

to be at $\phi = 97.0°$ while the average position of the [110] and [1$\bar{1}$0] directions suggests that the ϕ angle should be 97.6°.

The somewhat complex conclusion for the structures of this uranium film is that there are probably six different epitaxial domains for the uranium but that only four domains are observed in the experiment. The first two domains have the [$\bar{1}$10] uranium axis parallel to the tungsten [111] direction that is parallel to the sapphire [00.1] direction while in the other domains the uranium [110] is parallel to the other tungsten [111] directions. These domains are shown in the upper and lower parts of figure 7. The figure also shows that there is not a 2D lattice match with this relationship—the fit relates only to the spacings between the close-packed row atoms (and indeed ⟨111⟩ is not the closest-packed row of U).

These results are in contradiction with the results obtained for thin films of uranium on tungsten substrates [1, 2]. We do not understand the reason for this, but because of it we have not tried to optimize the growth to obtain a single domain for the tungsten substrate which presumably would then give a simpler set of structures for the uranium layer.

3.3. Niobium/gadolinium/uranium

The sample is described in table 1; the most intense scattering was the peaks from the sapphire substrate and these agreed with the previous measurements for the niobium buffer layers. The niobium and gadolinium buffers both gave clear peaks at wavevectors close to the (110) Bragg reflections of the niobium and the (00.2) Bragg reflections of the gadolinium. The wavevectors deduced from the niobium wavevectors were 2.703 ± 0.002 Å^{-1} and the gadolinium reflections had a wavevector of 2.174 ± 0.002 Å^{-1}. Both are in reasonable agreement with the values obtained from the bulk materials. Transverse mosaic spread scans were made of both of these reflections, and the results were $0.08 \pm 0.01°$ for the niobium and $0.50 \pm 0.02°$ for the gadolinium. This last result is substantially larger than the mosaic spreads for the first two samples.

In addition, two peaks were observed with wavevectors of 2.494 ± 0.002 Å^{-1} and 2.449 ± 0.002 Å^{-1}. Examination of table 2 suggests that the first of these reflections, which was about five times stronger, comes from the (021) planes of α-uranium while the second wavevector is from a smaller fraction of (110) planes. The mosaic spread of these reflections was measured with transverse scans and the results for both structures were $0.72 \pm 0.02°$.

The off-axis reflections were measured to confirm these structures and to determine the orientation of the layers. The niobium layer had off-axis (310) reflections consisting of a pair of reflections 180° apart, at angles of $\phi = 123°$ and 303°, showing that there is a single domain for the niobium buffer as expected. The wavevector of the niobium perpendicular to the growth direction was 2.651 ± 0.010 Å^{-1}, slightly less than the bulk crystal. The gadolinium is expected to have a hexagonal structure and this is confirmed in figure 8, which shows a regular sequence of repeating peaks in a ϕ scan through the (10.4) and (10.5) Bragg reflections. The results show peaks at values of $\phi = 2.9 + 60n$, where n is an integer, showing that one of the gadolinium (10.0) pairs of reflections is parallel to the unique niobium [1$\bar{1}$0] direction, whereas the other two gadolinium reflections are not parallel to any special direction in the niobium buffer. The length of the (10.0) wavevector of the gadolinium was determined as 1.965 ± 0.010 Å^{-1}, whereas that of the bulk material is 1.995 Å^{-1}, showing that the structure of the gadolinium layer is very similar to that of the bulk but slightly expanded along the a-axes.

The structure and orientation of the uranium layer was studied by measuring the (242) and (041) reflections for the (021) layers and the (223) reflections for the (110) layers. The results are summarized in figure 9, which shows the results of ϕ scans for the (041) and (223) reflections. The unexpected aspect is that there are (223) reflections which are strong and repeat every 180° but occur only for those ϕ angles corresponding to reflections aligned parallel to the niobium [1$\bar{1}$0] directions. The intensities corresponding to

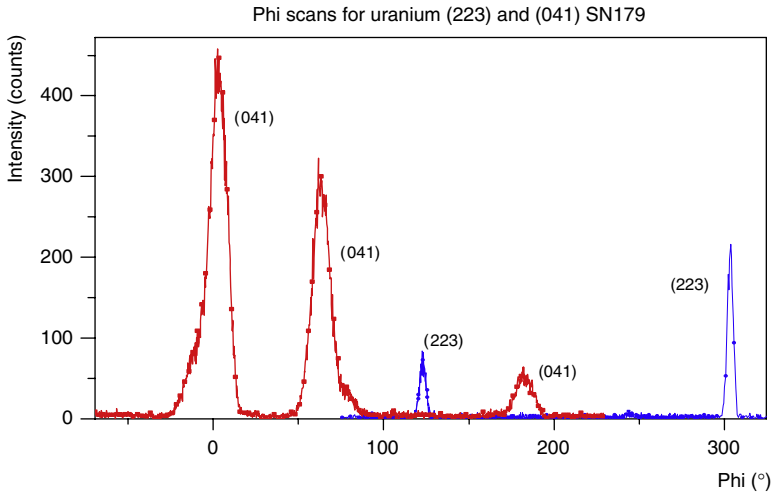

Figure 9. A ϕ scan of the (223) reflection from the (110) planes and of the (041) reflections of the (210) planes. Note the different ϕ angles obtained for the different structures.

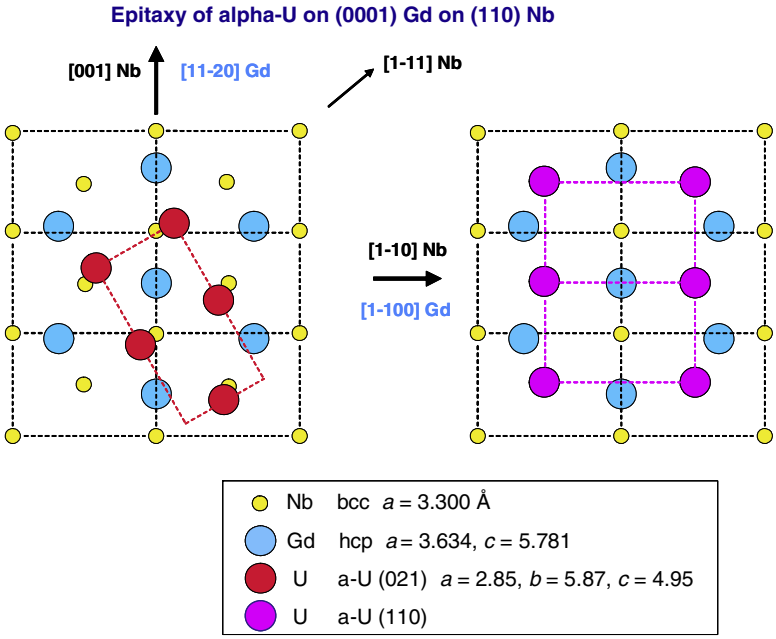

Figure 10. Schematic diagram showing the structures and orientations of the domains of U when grown on Gd.

other peaks from the (223) reflections are at least an order of magnitude smaller. In contrast, the (041) reflections show there are domains that are only oriented at the gadolinium reflections which do not correspond to the niobium [1$\bar{1}$0] directions. Analysis of the results for the (242) reflections gives the same conclusion. This behaviour of the domains is surprising because the gadolinium was 600 Å thick and we could not detect any difference in the in-plane lattice constants of the gadolinium reflections associated with the (021) uranium layers and the (110) uranium layers. Nevertheless, the multi-domain structure of the uranium is clearly closely connected with the underlying niobium buffer. It is also surprising that these two different epitaxial structures apparently have similar energies, because the scattered intensity from the (110) layers is similar to that from the (021) layers.

The transverse component of the (223) reflection gives a measure of the (001) lattice parameter for the (110) domain. The reciprocal lattice wavevector is 1.270 ± 0.020 Å^{-1} and can be compared with the bulk value given in table 1, namely 1.268 Å. The other (021) domain for the uranium has reciprocal lattice parameters of 2.19 ± 0.02 Å^{-1} for the (100) lattice parameter and 1.25 ± 0.02 Å^{-1} for (001) lattice parameter. Furthermore, the [001] and the growth direction were found to be at an angle of $59.3 \pm 1.0°$. These results are all compatible with the expected wavevectors and angles, including the angle, which is calculated to be 59.2° for bulk uranium. In figure 10 we show the unit cell perpendicular to the growth axis for both types of domain and also for the gadolinium substrate. There is a large lattice mismatch for both

types of domain and it is difficult to understand the origin of the epitaxial relationships. A schematic diagram of the gadolinium and uranium layers is shown in figure 10 but it is still hard to understand the epitaxial relationship and why there are the two different structures.

In conclusion, the α-uranium has three different domains. One domain has (110) planes stacked so that the [001] direction is parallel to the gadolinium [10.0] direction and to the niobium [1$\bar{1}$0] direction, whereas the other two domains have the uranium [041] direction oriented parallel to those gadolinium [10.0] directions that are not aligned with the underlying niobium [1$\bar{1}$0] direction.

4. Summary and conclusions

We have shown that epitaxial films of uranium with a thickness of at least 600 Å can be grown using a UHV sputtering facility in which the sample temperature can be controlled. Somewhat surprisingly, the structure and orientation of the uranium film depends critically on the nature of the substrate and the temperature of deposition. In most cases the uranium is deposited with the orthorhombic structure of α-uranium and the growth planes are (110) for a niobium (110) buffer, (002) for a tungsten (110) buffer and a mixture of (110) and (021) when the sample is grown on gadolinium (00.1) deposited on top of the niobium buffer. The lattice parameters and the orientational relationships of the epitaxial films are summarized in tables 3 and 4.

It is unusual to find when growing epitaxial films that the structure is so sensitive to the details of the substrate. This can be understood because there are many planes in α-uranium that have similar spacings (table 2), whereas in cubic semiconductors, for example, the spacings of the planes are very different from one another. We therefore conclude that similar results may be obtained in other systems of low symmetry that have many different planes with very similar spacings. Metallic bonding is also much more flexible than semiconductor bonding, allowing, as we have seen, epitaxial structures which have very large lattice mismatch.

These results differ from the results obtained earlier for thinner films of uranium [1, 2]. These all suggested that, when grown on tungsten, thin uranium films had a hexagonal phase. The difference with our results is that these films were much thinner, about 80 Å or less, and were annealed at high temperatures. We wonder if the complex and multiple structures described above were interpreted as arising from hexagonal uranium and we plan to investigate this further. It is complicated because we cannot use our in-house x-ray facility to measure the structure of 80 Å films reliably.

In conclusion we have shown that epitaxial layers of alpha-uranium can be grown by sputtering. This overcomes the problem of producing single crystals because they can be grown at lower temperature than with conventional growth from liquids and hence avoid cooling the material through the two high temperature phase transitions. The layers have been grown on several substrates constructed from sapphire and a refractory metal buffer. The results show that it is now possible to grow uranium films with different orientations, which could then be used for measurements of, for example, the photoemission or the structure of an oxygen layer so as to obtain more information about the electrical properties and the mechanism of the corrosion of uranium layers and how this depends on the surface plane. We hope that this will also enable further measurements of the electronic structure to be made to test whether these epitaxial structures become magnetic or have a charge density wave at low temperatures [8]. We hope that this research leads to a determination of the electronic structure of these unusual metals and we plan to further investigate other substrates to find new orientations and new phases of uranium metal.

Acknowledgments

We are grateful for helpful discussions with R Springell and M R Wells.

References

[1] Molodtsov S L, Boysen J, Richter M, Segovia P, Laubschat C, Gorovikov S A, Ionov A M, Prudnikova G V and Adamchuk V K 1998 *Phys. Rev.* B **57** 13241

[2] Berbil-Bautista L, Hanks T, Getzlaff M, Weisendanger R, Opahle I, Koepernik K and Richter M 2004 *Phys. Rev.* B **70** 113401

[3] Beesley A M, Thomas M F, Herring A D F, Ward R C C, Wells M R, Langridge S, Brown S D, Zochowski S W, Bouchenoire L, Stirling W G and Lander G H 2004 *J. Phys.: Condens. Matter* **16** 8491
Beesley A M, Thomas M F, Herring A D F, Ward R C C, Wells M R, Langridge S, Brown S D, Zochowski S W, Bouchenoire L, Stirling W G and Lander G H 2004 *J. Phys.: Condens. Matter* **16** 8507

[4] Springell R, Zochowski S W, Ward R C C, Wells M R, Brown S D, Bouchenoire L, Wilhelm F, Langridge S, Stirling W G and Lander G H 2007 *Preprint* 0704.3947
Springell R, Zochowski S W, Ward R C C, Wells M R, Brown S D, Bouchenoire L, Wilhelm F, Langridge S, Stirling W G and Lander G H 2007 *Preprint* 0704.3970

[5] Wilhelm F, Jaouen N, Rogalev A, Stirling W G, Springwell R, Zochowski S, Beesley A M, Brown S D, Thomas M F, Lander G H, Langridge S, Ward R C C and Wells M R 2007 *Phys. Rev.* B **76** 024425

[6] Ward R C C, Grier E J and Petford-Long A K 2003 *J. Mater. Electron.* **14** 533

[7] Wyckoff R 1965 *Crystal Structures* 2nd edn, vol 1 (New York: Interscience)

[8] Lander G H, Fisher E S and Bader S D 1994 *Adv. Phys.* **43** 1–111